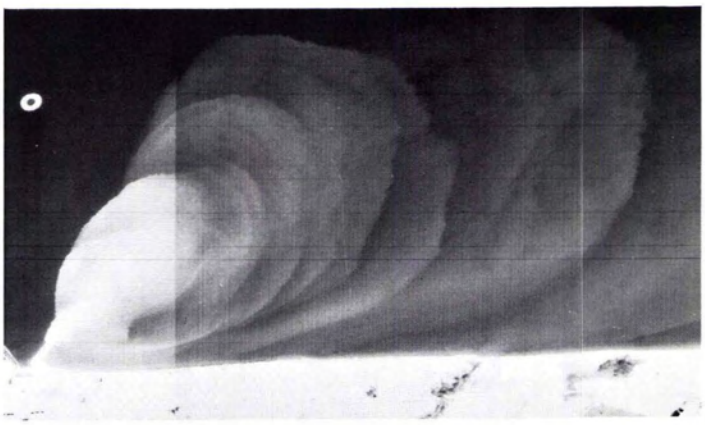

FRONTISPIECE Thermal imagery of Point Beach power plant, 15 September 1971, H = 660m.

DR. F. L. SCARPACE
DR. R. P. MADDING
DR. T. GREEN III
University of Wisconsin
Madison, WI 53706

Scanning Thermal Plumes*

The temperature and temperature gradient of power plant thermal plumes were determined employing an airborne thermal scanner.

INTRODUCTION

IN SPITE OF the lack of knowledge of the behavior and effects of the "thermal plumes" associated with the condenser cooling of power plants, far-reaching plant siting decisions are now being made on the basis of the little existing data. Despite their small size, these thermal plumes are much more difficult to characterize than most people realize. Over 800 thermal line scans of power plant plumes taken during the past three years indicated that their mixing with the nearshore lake water is extremely complex and highly dependent on environment conditions. Thorough knowledge of the mixing process can be obtained only from data acquired over the areas of interest for a long period of time under a variety of weather conditions.

A cooperative effort to monitor all thermal plumes along the Wisconsin shore of Lake Michigan has been undertaken. The program is jointly sponsored by the State of Wisconsin Department of Natural Resources (DNR), the University of Wisconsin-Madison, and three power companies: Wisconsin Power and Light, Wisconsin Public Service Corporation, and Wisconsin Electric Power Company. The thermal scanning data acquisition is under the direction of the University.

Since December 1972, thermal line scans of all the major power plants in the State of Wisconsin have been acquired on a twice weekly basis. The flight path is indicated in Figure 1. The aircraft used for the operational program is a DC-3, owned by the Wisconsin DNR and specially equipped with an area navigation system, TV monitoring system, and a mapping camera. A Texas Instruments (TI) RS-18A scanner is used. A block diagram of the scanning system can be found in Figure 2. Examples of thermal scans for each of

* Contribution No. 28 of the Marine Studies Center, University of Wisconsin, Madison.

the six operating power plants that are monitored are shown in Figures 3 and 4.

Routine ground truth is gathered by the power companies. Both hot and cold temperatures are measured at each of the plants during each flight. At some of the plants surface water temperatures were measured by using thermometers; at other plants recorded thermocouple intake and discharge temperatures were used. The utility companies also have provided monies for scanning equipment and partial funding of flight time for the DC-3.

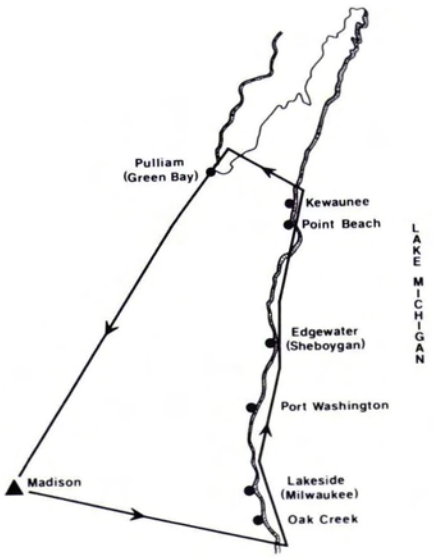

FIG. 1. Flight path for routine thermal scanner flights. The solid line indicates the round trip flight path to thermally scan seven operating power plants and selected areas of Lake Michigan shoreline.

THERMAL PLUMES

An overview of the techniques used at the University of Wisconsin for analyzing thermal scanner data as applied to the imagery from the Point Beach power plant at Two Creeks, Wisconsin (on Lake Michigan) is described below. The plant has two 500-Mw (megawatt) units with once-through condenser cooling. The cooling water is discharged through two open flumes (11 meters

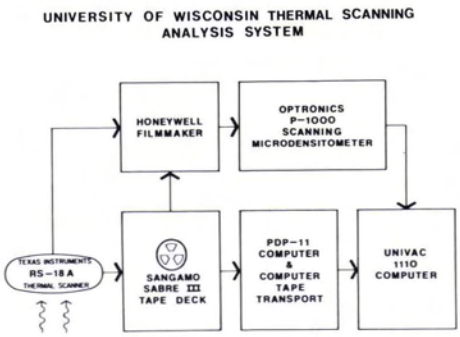

FIG. 2. Block diagram of the thermal scanning data acquisition and analysis system at the University of Wisconsin.

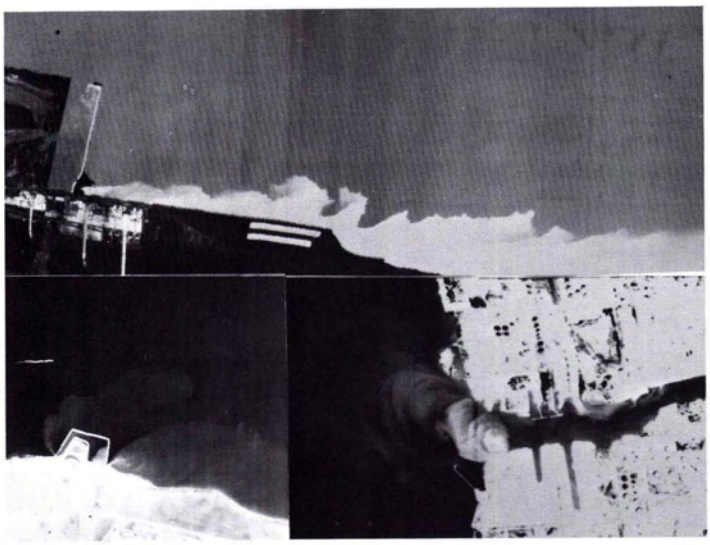

FIG. 3. Top: Oak Creek, 11 January 1974; flying height (H) = 330m. Bottom Left: Lakeside, 15 May 1974; H = 660m. Bottom Right: Pulliam, 10 July 1973; H = 1000m.

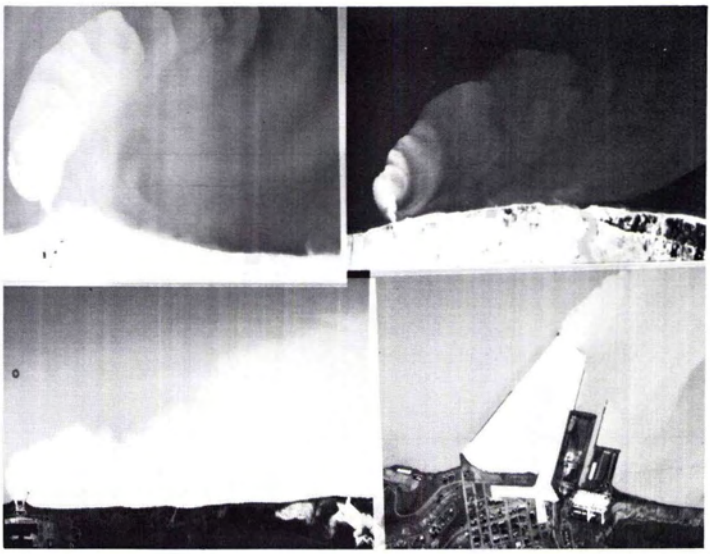

FIG. 4. Top Left: Kewaunee, 15 May 1974; H = 1000m. Top Right: Edgewater, 15 May 1974; H = 660m. Bottom Left: Point Beach, 23 April 1974; H = 600m. Bottom Right: Port Washington, 23 April 1974; H = 660m.

wide and about 3 meters deep) at 350,000 gallons-per-minute each, and is usually about 10°C warmer than water at the offshore plant intake. The outfall densimetric Froude number is about 10; the outfall Reynolds number is about 2×10^6.

With the routine flights, numerous lower-altitude missions were flown at the Point Beach plant. (Four-hundred scans of this plume have been acquired.) During the low-altitude flights, more detailed ground truth was gathered by University personnel. Sequential imagery of the plume was recorded for time periods of up to two hours. This allows an analysis of short-term variations in the surface temperature of the plume.

On relatively calm days, a series of concentric thermal fronts is apparent on the imagery. The Frontispiece shows imagery from such a day. The motion of the fronts can be traced on successive thermal images resulting in a vector plot of the velocity of the thermal fronts (Figure 5). The front velocities are somewhat greater than water velocities observed on other days by aerial photographic techniques. A more detailed analysis of these data will be reported elsewhere.

On several days when the plane was overhead, a boat with a PRT-5 radiometer mounted on its bow was making transects of the plume. Since the radiometer measures surface temperature in a manner similar to that of a thermal scanner, it is the ideal instrument to use for ground truth measurements. The boat passes over a predetermined course marked by 20 buoys. It starts at the outer buoys, so as not to disturb parts of the plume to be measured later. The boat takes approximately 30 minutes to make one complete circuit of the buoy pattern.

Figure 6 shows contours drawn from the data taken on the same day as the imagery for the Frontispiece was flown. Note that the thermal fronts, so obvious on the synoptic thermal imagery acquired this day, do not appear. Because of the rapid variation in the plume, the non-synoptic boat measurements seem to provide an inadequate description of the temperature structure of this plume in some cases.

Since temperature gradients may be as or more important biologically than the absolute temperature, a measure of the plume sur-

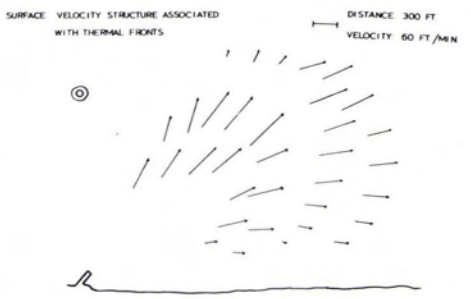

FIG. 5. Surface velocity structure associated with thermal plumes.

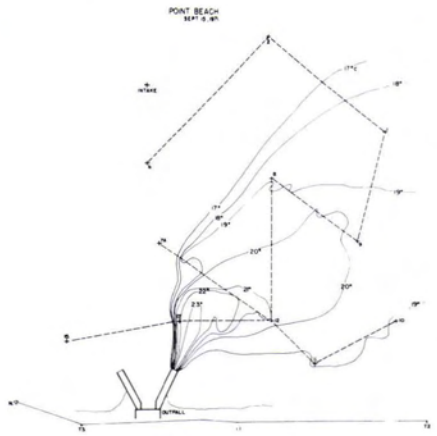

FIG. 6. Surface isotherms drawn from boat transects. Dashed line indicates the boat path.

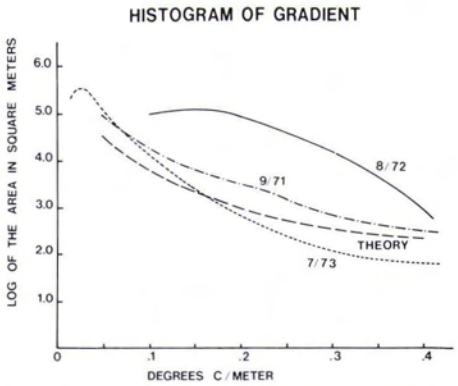

FIG. 7. Graph of surface area covered by horizontal temperature gradients.

face area covered by absolute horizontal gradients of various strengths may be of interest. The horizontal temperature gradients are computed by using centered finite differences on the thermal scanning imagery.[1] Subsurface temperature measurements using thermistors showed the gradients to persist to three meters below the surface.[1] Gradients have been found in the plume in excess of 1.6°C/meter. This is a lower bound on the maximum gradient. The maximum gradient calculated depends on the resolution of the thermal scanning system. Boat-mounted PRT data show much larger gradients.

Graphs of surface area covered by absolute horizontal gradients of various strengths can be plotted. Figure 7 shows an example of such a graph for three different days. Also plotted is a theoretical prediction based upon the assumption that the surface temperature has a Gaussian distribution normal to the plume center line, and that the temperature decreases with the inverse square root of the distance along the center line.[2] Some of the measured graphs differ from the model by a factor of 10.

Although the size and shape of the thermal plume changes quickly in response to changing plant load and changing environmental conditions, a few kinds occur sufficiently often to be recognized as distinct types of surface plumes. In general, most of the plumes can be classified as either a "normal," a "rough-water," a "front-laden," or a "meandering" plume. Examples are shown in Figures 8 and 9. "Rough-water" and

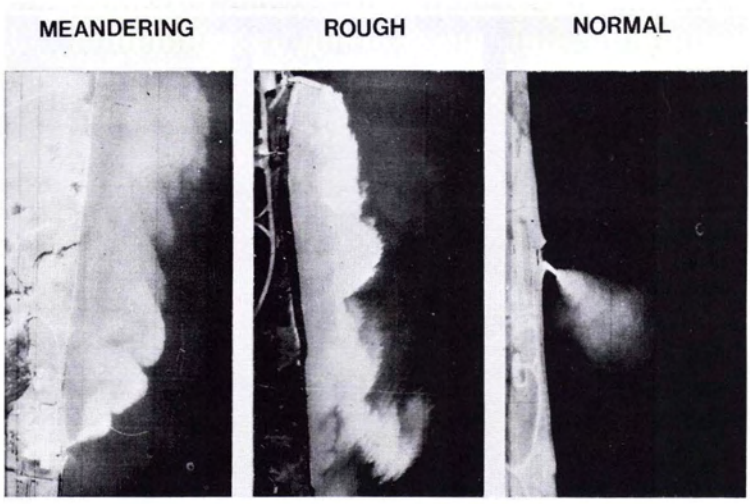

FIG. 8. Point Beach thermal plumes showing three of the five types.

"meandering" plumes are similar in nature, except the "meandering" plume's "periodic" structure and edge definitions persist for several miles from the discharge. With a sufficiently broad interpretation, the above plume types encompass about 90 per cent of the data. Most of the other plumes defy classification, such as the "changing" plume in Figure 9, and seem to be associated with changing environmental conditions. Work is in progress to correlate these plume types to plant load and wind and wave conditions.

Another parameter that can be correlated with the plant load and environmental conditions is the centroid of the plume. In this case the plume was taken as the visible extent of the mixing zone on the film imagery. This corresponded to approximately the one-degree-centigrade-above-ambient isotherm. This is not as accurate as using the data directly from the tape recorder, but the cost of analysis is considerably less. Figure 10 gives an example of a centroid vector and the outline of the plume as drawn by a computer. Table 1 is a summary of other plumes analyzed in this fashion.

Temperature Dependence of Thermal Scanner

The signal out of a thermal scanning system can be written as:

$$V = A \cdot \int E(\lambda) \cdot F(\lambda) \cdot S(\lambda) d\lambda + B \quad (1)$$

where $E(\lambda)$ is the energy arriving at the scanner in the field of view
$F(\lambda)$ is the optical transmission factor of the scanning system
$S(\lambda)$ is the relative sensitivity of the detector
A is the system gain
B is the offset voltage
V is the output voltage (signal)

and the integral is overall positive values of the wavelength λ. The energy arriving at the scanner is dependent on three things: the temperature of the ground object, the emissivity of the object, and the atmospheric modification of the emitted energy from the ground. Atmsopheric modification of the signal is discussed later in the paper. To assign an apparent temperature to the energy arriving at the scanner, Equation 1 can be rewritten as:

$$V = A' \epsilon G(T) + B \quad (2)$$

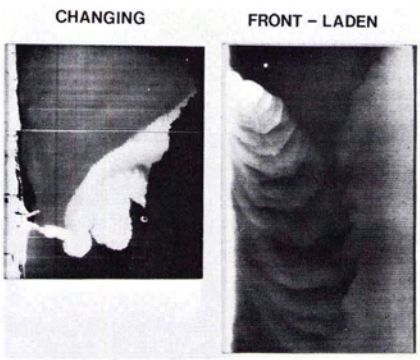

Fig. 9. Point Beach thermal plumes showing two of the five types.

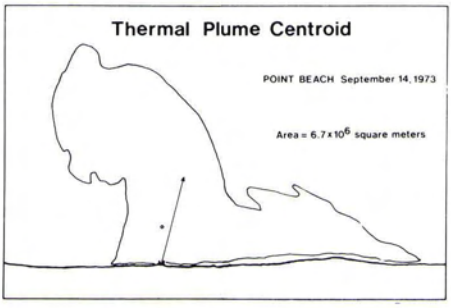

Fig. 10. Thermal plume outline including centroid vector.

Table 1. Area and Centroid of Some Point Beach Thermal Plumes.

Date (1973)	Surface Wind		Waves		Area	Centroid		Crab Angle
	Knots	Direction	Meters	Direction	$m^2 \times 10^{-6}$	$m \times 10^{-2}$	Heading	
23 March	10	SE	0.3	SE	2.56	23	21°	2°
28 March	—	—	—	—	1.77	17	15°	4°
17 April	26	SE	0.6	SE	2.68	26	23°	5°
10 July (10:05)	10	NNE	calm	—	1.87	15	163°	5
10 July (13:50)	8	ENE	calm	—	1.55	13	169°	7°
11 July	3	NE	0.3	SE	5.30	19	162°	6°
14 Sept.	2	NE	0.6	SE	6.73	12	107°	2°

where $G(T)$ includes an integral over all wavelengths of Planck's distribution times the functions $F(\lambda)$ and $S(\lambda)$, and ϵ is the emissivity. This will be a reasonable approximation to the signal emitted by the ground if the atmosphere is a linear attenuator and emissivity is a constant over the band pass of the system. Neither of these is strictly true, but if the functional dependence is known, they can be incorporated into the function $G(T)$.

The measured quantity for scanning systems is V. The constants A' and B must be known or calibrated in flight with ground truth. Thus, if ϵ for the object and the functional dependence of G is known or assumed, the temperature can be found.

The values of the integral in Equation 2 for the RS-18A scanner were calibrated for all values of temperature between 0°C. Various functional dependences of temperature were investigated in order to find the best fit. Errors associated with each assumed functional dependence were calculated. Note that the errors are valid only for the University of Wisconsin's RS-18A since $F(\lambda)$ and $S(\lambda)$ are scanner dependent.

The function dependences investigated were:

$$\begin{aligned} G(T) &= A + B\,T \\ &= A + B\,T^4 \\ &= A + B\,T + C\,T^2 \\ &= A + B\,T + C\,T^2 + D\,T^3 + E\,T^4 \end{aligned}$$

The errors associated with these assumed dependences on temperature are shown in Figure 11. These plots are for a temperature range of the data of 30°C. For a temperature range of 20°C the errors are approximately one-half of the plotted errors.

A two-point ground calibration of a thermal scanning system using this method proceeds as follows:

(1) The voltage for two known temperatures must be known (from ground truth measurements).
(2) The parameters for the $G(T)$ are calculated for the temperature range desired.
(3) The value of G is calculated for the known temperatures.
(4) Constants A and B then can be calculated from the known V's and G's.
(5) The apparent temperature for any other voltage can then be calculated.

By using these methods, it is possible to eliminate errors due to the functional dependence of the incoming radiation. As can be seen from Figure 11, the normal assumption of a T^4 dependence is sufficient for most purposes (over short ΔT's).

Modulation Transfer Function

The intrinsic modulation transfer function (MTF) of our RS-18A scanner was calculated from bench test results. A thermal step function was input to the scanner using a hotplate partially masked with a cold metal sheet. A three-meter focal length spherical mirror was used to insure that the incoming radiation acted like a source at infinity. The output voltage is depicted in Figure 12. The 100 percent rise time is about 20 microseconds. Digital time series analysis techniques using Fast Fourier Transforms were applied to this trace. The resultant system transfer function is shown in Figure 13.

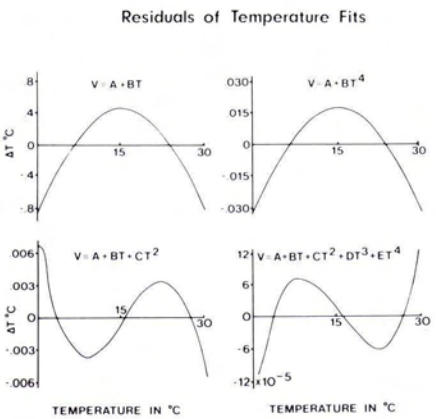

Fig. 11. Residuals of temperature fits.

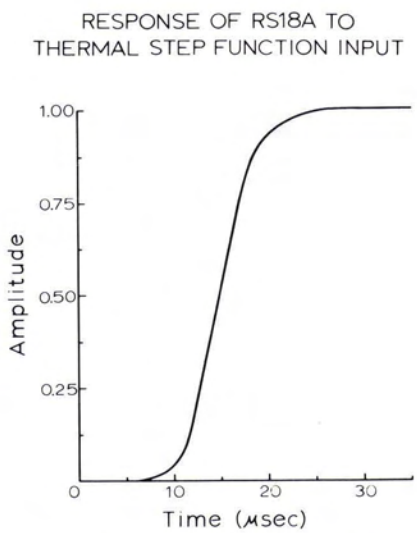

Fig. 12. Output response of RS-18A thermal scanner to a thermal step function input.

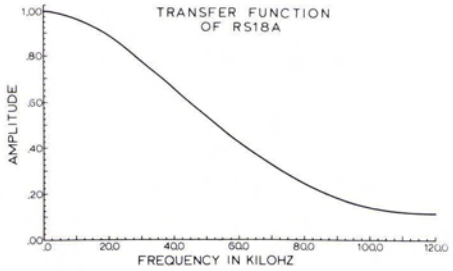

FIG. 13. Transfer function of RS-18A thermal scanner.

Typically, the quoted resolution of scanning systems is based on the minimum resolution for which differences can be detected on a photographic image of the data, about a 30 per cent MTF. For surface water temperature measurements, isothermal regions at least as large as the area swept by the detector in the 100 per cent rise time must exist. For the RS-18A scanner this corresponds to an instantaneous field of view for the detector of 10.5 milliradians. Since this is an area of about four times as large as the typically stated resolution for this scanner, *caution must be exercised when assigning ground truth temperatures to the imagery.* Further work is being done to apply the transfer function using Fourier Transform techniques to the digitized scanner output data. By convoluting the scanner output with the MTF, a more nearly correct image of the input may result.

CALIBRATION

In order to ascertain the degree of confidence in the analysis techniques, thermal scanner laboratory and field calibration tests are necessary. On some of the low-altitude flights during the summer of 1973 and winter of 1974 detailed thermal calibrations were conducted at the Point Beach site. Tests were performed on both the Wisconsin RS-18A thermal scanner and the National Center for Atmospheric Research (NCAR) TI RS-310 thermal scanner. Thermal ground truth was obtained by monitoring the temperature of stirred water in several 3-meter-diameter swimming pools as well as one lake temperature. (The stirring eliminates the surface skin temperature effect.) Figure 14 is a film image of one of the RS-18A scans made on 10 January 1974. Figure 15 is a computer character representation of the temperature of the area enclosed by the white rectangle in Figure 14 showing the pools (P1, P2 and P3). Aluminum sheets (outlined, but not labelled) were placed beside each pool to facilitate identification. P4 is a wader monitoring the lake temperature.

The computer printout is derived from digitizing the output voltage of the scanning system into 256 levels. Using the temperatures measured at P1 and P4, a two-point calibration was performed. The functional dependence on the input radiation was assumed to be $A + BT^4$, where T is surface temperature and A and B are constants (see discussion above as to the method). As a consistency check, a least squares fit to the data was performed. Results are detailed in Table 2. It should be noted that the outfall temperature could not be used as a calibration point because a thin layer of fog was present just above the hottest part of the plume; further, pool P2 partially collapsed and the temperature data were unusable.

Geometric ground truth was provided by aerial photographs and strategically located aluminum sheets. These sheets appear as

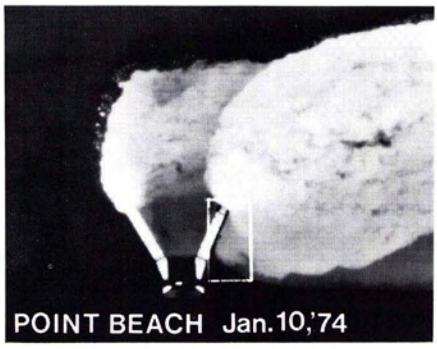

FIG. 14. Thermal imagery of a 210-meter altitude pass over Point Beach. The white rectangle outlines the approximate area covered by Figure 15.

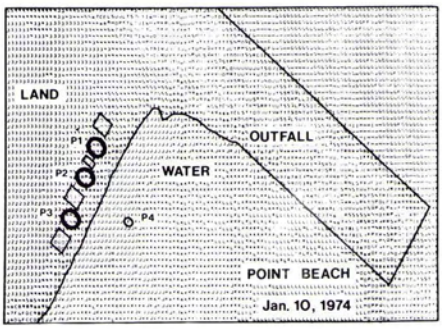

FIG. 15. Computer printout of a digitized thermal image. The area covered is enclosed by a white rectangle in Figure 14. The 3-meter-diameter swimming pools are labelled P1, P2 and P3. P4 is a man wading in the lake.

TABLE 2. RESULTS OF LEAST SQUARES FIT TO $V = A + BT^4$.

Location	Measured Temperature °C	Calculated Temperature °C	Deviation °C
P1	0.0	−0.07	−0.07
P3	0.4	+0.47	+0.07
P4	9.55	9.55	0.00

cold spikes in the imagery due to their low emissivity. The average ground speed between any two of these ground control points can be readily calculated allowing us to rectilinearize the imagery to better than 2 per cent including the taking out of effects of the crab of the aircraft (i.e., the angle between aircraft centerline and direction of flight caused by crosswinds).

Removal of crab on computer printouts becomes a problem due to the large number of data points involved. Other effects such as tangential distortion and ground speed variation can be removed on a line-by-line basis involving approximately 700 data points. However, crab removal can involve as many as 100 scan lines requiring remapping an array of 70,000 elements. A contouring program has been developed to remove the crab from measurements on the computer printout of the scanned area. Figure 16 shows the results of this procedure.

During some of our flights using the NCAR thermal scanner, the dry bulb temperature, wet bulb temperature, and static pressure were recorded continuously on board the aircraft. Soundings down to 16 meters above the lake were made in order to obtain sufficient data to numerically integrate the radiation transfer equation over the wavelength range of 8 to 14 microns. The numerical integration was based on a computer program written by Cox[3] who used the Elsasser and Culbertson model.[4] Water and carbon dioxide were the only absorbers accounted for; the effects of aerosols were neglected.

A typical mid-summer sounding (mixing ratio of about 8 grams water/kilogram of dry air) done on 10 August 1973 indicated an attentuation in radiation intensity of about 3.5 per cent at an altitude of 1520 meters. At this altitude the difference in intensity between a 0° scan angle and a 50° scan angle was about 0.13 per cent. For a ground temperature of 22°C this corresponds to an apparent temperature at 1520 meters of 19.5°C at 0° scan angle. 19.4°C at 30° scan angle, and 19.0°C at 50° scan angle.

Larger apparent temperature differences between the nadir and the 50° scan angle have been observed. These occurrences have

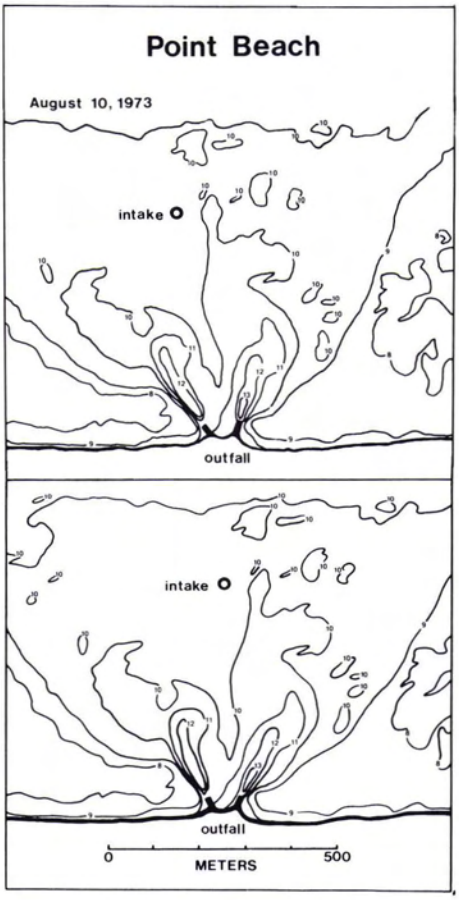

FIG. 16. Surface temperature isotherms (in °C) generated from a digitized thermal image. The upper contour is not crab-correlated; the lower contour is crab-corrected.

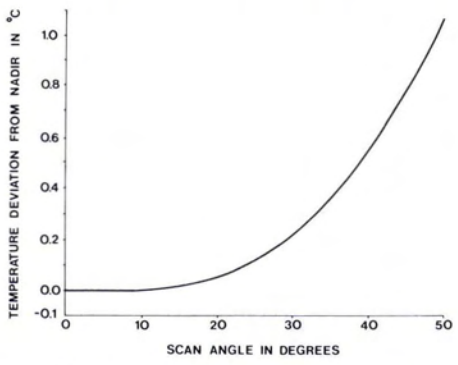

FIG. 17. Temperature deviation versus scan angle. The thermal image was recorded on 23 July 1973 at an altitude of 1520 meters above a 6°C isothermal region of Lake Superior.

been infrequent and occur on days of high humidity and haze. The largest difference observed has been 1.05°C. This occurred over an isothermal (6°C) section of the surface of Lake Superior on a warm day (23 July 1973). The isothermal nature of the lake surface was verified by water surface measurements from a boat, and overlapping thermal scanner flight lines. Figure 17 is a trace of the output voltage for one-half a scan line on this day. The figure indicates an increase in apparent temperature with increasing scan angle. This unusual effect has been noted only twice during the past two years. It was probably due to the very warm moist air over the cold lake. Fog had been a recurring problem throughout the day; the scan was done during one of the apparent breakups that occurred. For low enough altitude soundings, integration of the radiation transfer equation can predict such an effect.

The atmospheric sounding can be used to assign surface temperature to the thermal imagery, if one can assure atmospheric conditions to be horizontally uniform. Ground truth compensates for the atmospheric attentuation effects at the corresponding scan angle, then the atmospheric model compensates for the change in apparent temperature due to scan angle. The atmospheric model is not used for absolute calibration of the scanning system (i.e., using the calibrated black body sources in the scanner) because small errors in calculated attenuation of intensities can result in large errors in calculated temperatures. This is likely because the functional dependence of the output depends on the absolute temperature of the source of the emitted energy.

Conclusion

Obtaining quantitative surface-temperature data from thermal scanning systems is a nontrivial task. Great care is needed in order to achieve accuracies of ±0.1°C, but it can be done with carefully taken ground truth. For routine monitoring, such care is probably not warranted. For efforts to understand the dynamics of such plumes, it is warranted. The user of scanning data should make a conscious choice of the level of ground truth effort, based upon the accuracies he needs.

Acknowledgments

The authors wish to thank Mr. Gerald Friederichs, Mr. John Rogers and Mr. Robert Walker for their invaluable assistance in data acquisition and computer programming.

This research was supported in part by the Wisconsin Department of Natural Resources, Wisconsin Power and Light Company, Wisconsin Public Service Corporation, Wisconsin Electric Power Company, National Aeronautics and Space Administration Office of University Affairs, National Oceanic and Atmospheric Administration's Office of Sea Grant, U. S. Department of Commerce, and the National Science Foundation through a RANN Grant to the Institute for Enyironmental Studies at the University of Wisconsin.

References

1. F. L. Scarpace and T. Green III, *Water Resources Research*, Vol. 9, No. 1 Feb. 1973.
2. Koh and Fan, Mathematical Models for the Prediction of Temperature Distributions Resulting from the Discharge of Heated Water into Large Bodies of Water, Environmental Protection Agency Technical Report #16130DW010/70, p. 1-219, Washington, DC, October 1970.
3. S. K. Cox, private communication.
4. W. M. Elsasser and M. F. Culbertson, *Meteorological Monograph*, Vol. 4, No. 23, August 1960.
5. F. L. Scarpace, R. P. Madding, and T. Green III, *Proceedings of the 9th International Symposium on Remote Sensing of Environment*, Univ. of Michigan, April 1974, pp. 939-961.

Important Notice
Nominations for Society Officers

The ASP Nominations Committee has been constituted with Prof. Dean C. Merchant as Chairman. Other members of the Committee are Mr. Arnold Lanckton and Dr. Robert Turpin.

Each year, by precedent, the Society alternately draws its nominations from either industry or government and the educational community. For the 1976 election of officers, candidates will be drawn from members associated with government agencies at the federal, state, and local levels.

The ASP By-Laws provide that any regular member in good standing may nominate other members to be officers of the Society. Nominations and supporting information should be sent to: Prof. Dean C. Merchant, Chairman, ASP Nominations Committee, Dept. of Geodetic Science, The Ohio State University, 1958 Neil Avenue, Columbus, Ohio 43210.